



THE UNIVERSITY *of* EDINBURGH

Edinburgh Research Explorer

An intrinsic S/G checkpoint enforced by ATR

Citation for published version:

Saldivar, JC, Hamperl, S, Bocek, MJ, Chung, M, Bass, TE, Cisneros-Soberanis, F, Samejima, K, Xie, L, Paulson, JR, Earnshaw, WC, Cortez, D, Meyer, T & Cimprich, KA 2018, 'An intrinsic S/G checkpoint enforced by ATR', *Science*, vol. 361, no. 6404, pp. 806-810. <https://doi.org/10.1126/science.aap9346>

Digital Object Identifier (DOI):

[10.1126/science.aap9346](https://doi.org/10.1126/science.aap9346)

Link:

[Link to publication record in Edinburgh Research Explorer](#)

Document Version:

Peer reviewed version

Published In:

Science

Publisher Rights Statement:

* This manuscript has been accepted for publication in Science. This version has not undergone final editing. Please refer to the complete version of record at <http://www.sciencemag.org/>. The manuscript may not be reproduced or used in any manner that does not fall within the fair use provisions of the Copyright Act without the prior, written permission of AAAS.

General rights

Copyright for the publications made accessible via the Edinburgh Research Explorer is retained by the author(s) and / or other copyright owners and it is a condition of accessing these publications that users recognise and abide by the legal requirements associated with these rights.

Take down policy

The University of Edinburgh has made every reasonable effort to ensure that Edinburgh Research Explorer content complies with UK legislation. If you believe that the public display of this file breaches copyright please contact openaccess@ed.ac.uk providing details, and we will remove access to the work immediately and investigate your claim.



An intrinsic S/G2 checkpoint enforced by ATR

Authors: Joshua C. Saldivar¹, Stephan Hamper¹, Michael J. Bocek¹, Mingyu Chung¹, Thomas E. Bass², Fernanda Cisneros-Soberanis^{3,4}, Kumiko Samejima³, Linfeng Xie⁵, James R. Paulson⁵, William C. Earnshaw³, David Cortez², Tobias Meyer¹ and Karlene A. Cimprich^{1*}

Affiliations:

¹ Department of Chemical and Systems Biology, Stanford University School of Medicine, 318 Campus Drive, Stanford, CA 94305-5441, USA.

² Department of Biochemistry, Vanderbilt University School of Medicine, 2215 Garland Avenue, Nashville, TN 37232, USA.

³ Wellcome Centre for Cell Biology University of Edinburgh, King's Buildings, Max Born Crescent Edinburgh EH9 3BF, Scotland, UK.

⁴ Unidad de Investigación Biomédica en Cáncer, Instituto de Investigaciones Biomédicas - Universidad Nacional Autónoma de México; Insituto Nacional de Cancerología, México City 14080, Mexico.

⁵ Department of Chemistry, University of Wisconsin-Oshkosh, 800 Algoma Blvd, Oshkosh, WI 54901, USA.

* Correspondence to: cimprich@stanford.edu

Abstract:

The cell cycle is strictly ordered to ensure faithful genome duplication and chromosome segregation. Control mechanisms establish this order by dictating when a cell transitions from one phase to the next. Much is known about control of the G1/S, G2/M, and metaphase/anaphase transitions, but there is no known control mechanism for the S/G2 transition. Here, we show cells transactivate the mitotic gene network as they exit S phase through a CDK1-directed FOXM1 phosphorylation switch. During normal DNA replication, the checkpoint kinase ATR is activated by ETAA1 to block this switch until S phase ends. ATR inhibition prematurely activates FOXM1, deregulating the S/G2 transition and leading to early mitosis, under-replicated DNA and DNA damage. Thus, ATR couples DNA replication with mitosis and preserves genome integrity by enforcing an S/G2 checkpoint.

One Sentence Summary:

ATR represses a mitotic gene network until the S/G2 transition ensuring completion of DNA replication.

Main Text:

To avoid loss of genetic information, cells must replicate their DNA before mitosis (1). Recent data show replication delays the onset of mitosis (2), yet how cells sense the end of S phase and coordinate these processes remains a fundamental biological question. A checkpoint monitoring the end of DNA replication has been proposed (3), but effectors of such an S/G2 checkpoint have not been identified. DNA damage can activate the checkpoint kinase ATR (ATM and Rad3-related) arresting S or G2 cells by inactivating the CDC25-cyclin dependent kinase (CDK) pathway (4). Because ATR ensures completion of replication before mitosis during normal proliferation (5, 6), we hypothesized it may regulate the S/G2 transition.

To test this hypothesis, we used quantitative image-based cytometry (QIBC) (fig. S1) (7) combined with pulse-chase assays (fig. S2) and measured S-M and G2-M progression. S phase cells treated with ATR inhibitors (ATRi) underwent accelerated mitotic entry (Fig. 1, A and B). Surprisingly, ATR inhibition in G2 did not accelerate mitotic entry rates, whereas WEE1 inhibition did (Fig. 1C). This extends previous findings (5, 6) suggesting ATR acts in S phase and not G2 of normal cell cycles to delay mitosis.

These observations are consistent with ATR inhibition shortening S phase. Nevertheless, a pulse-chase-pulse assay (fig. S3) and live-cell imaging with an EYFP-PCNA biosensor (8) (fig. S4) revealed S-phase-shortening alone cannot explain the combined shortening of S and G2 following ATR inhibition (fig. S3, B-D). We hypothesized ATR controls subsequent G2 duration by delaying accumulation of pro-mitotic factors (9). Notably, inhibiting ATR led to premature cyclin B protein accumulation in S phase (Fig. 1, D-F and fig. S5). Moreover, ATR inhibition prematurely increased cyclin B1 mRNA in early S phase-synchronized cells, whereas in mock-treated synchronized cells, cyclin B mRNA increased concomitantly with the S/G2 transition

(Fig. 1G and fig. S6). To determine whether ATR similarly controls the transcription of additional genes, we performed RNA-seq. Unsupervised clustering analysis of sequenced reads revealed a group of genes prematurely upregulated with ATRi in S phase (Fig. 1H group 5, fig. S6E, and Table S1). Consistent with their normal G2 expression, GO-term analysis of group 5 showed enrichment for pro-mitotic factors (Fig. 1, I and J). These findings suggest a G2/M gene network poised for transcription in S phase but repressed by ATR until G2.

Next, we analyzed publically-available ChIP-seq data for transcription factor enrichment at the promoters of group 5 genes. Notably, B-MYB and FOXM1, transactivators of a mitotic transcription program (*10, 11*), were highly enriched at these sites (fig. S7A). We asked whether knockdown of either would prevent premature cyclin B accumulation. B-MYB knockdown caused a G1 arrest, precluding further study (fig. S7, B-D). Importantly, FOXM1 knockdown, which did not block S phase entry, prevented premature cyclin B accumulation in ATR-inhibited cells (fig. S7, B and E), confirming FOXM1 drives premature cyclin B expression.

To determine whether ATR regulates B-MYB and FOXM1, we monitored their phosphorylation, a requirement for their activation (*11, 12*). Whereas both proteins normally exhibit a profound phosphorylation shift at the S/G2 transition, ATR inhibition in early S phase triggered immediate hyper-phosphorylation (Fig. 2, A and B, and fig. S7F). In asynchronous cells, single-cell QIBC analysis revealed that FOXM1 T600 phosphorylation (fig. S8A), a CDK-dependent activating modification (*12*), rises in early S phase, then again in G2. Strikingly, ATR inhibition caused rapid and premature FOXM1 phosphorylation throughout S phase, raising pFOXM1 to G2 levels (Fig. 2, C-F, and fig. S8B-D). This premature phosphorylation occurred even after blocking replication with thymidine (fig. S9A). Moreover, mRNA FISH analysis of FOXM1 target PLK1, revealed that ATRi induced its premature expression with or without

thymidine (fig. S9, B and C). Thus, ATR suppresses FOXM1 phosphorylation and downstream transcription in S phase cells irrespective of S phase progression.

The marked difference in S- and G2-phase pFOXM1 levels suggests a specific regulatory event defines the S/G2 transition. Thus, we measured pFOXM1 levels during late S, the S/G2 transition (fig. S10), and early G2. pFOXM1 levels rose abruptly in the S/G2 population (Fig. 2, G and H), a finding confirmed using EYFP-PCNA and pFOXM1 imaging (fig. S11, A and B). As this population comprises less than 4% of the late S and early G2 cells, phosphorylation is switch-like in that it happens rapidly at the S/G2 transition.

Paradoxically, cyclin A-CDK phosphorylates FOXM1 (*12*), but total cyclin A-CDK activity gradually increases throughout S phase (*13*), inconsistent with switch-like behavior. To test whether a specific cyclin A-CDK complex mediates this behavior, we measured pFOXM1 levels following either CDK2 or CDK1 inhibition. CDK2 inhibitors had little effect on FOXM1 phosphorylation (Fig. 3, A and B and fig. S12A) although they decreased EdU incorporation (fig. S12B). In striking contrast, CDK1 inhibition prevented FOXM1 phosphorylation at the S/G2 transition and following ATR inhibition (Fig. 3, A and C, and fig. S12). Furthermore, analog-sensitive CDK1 (CDK1-as) inhibition (*14*) reduced FOXM1 phosphorylation, and CDK2 inhibition had no additional effect (fig. S13). These results show CDK1 phosphorylates FOXM1 at the S/G2 transition.

Given that ATR suppresses FOXM1 phosphorylation until G2, we hypothesized that ATR activity may abruptly decline as S phase ends, relieving an intrinsic checkpoint. Consistent with this hypothesis, ATR-dependent H2AX phosphorylation (γ H2AX) increased as cells entered S phase, peaked in mid-S phase, and rapidly decreased as cells completed DNA replication (Fig.

3, D and E, and fig. S14, A-D). Thus, ATR is active throughout normal S phase, but its activity drops at the S/G2 transition allowing rapid FOXM1 phosphorylation.

In mammalian cells, either a RAD9A-TOPBP1 or ETAA1-dependent pathway activates ATR (4). ETAA1 knockdown reduced ATR activity in an unperturbed S phase whereas RAD9A knockdown did not, even though it reduced γ H2AX following replication stress (Fig. 4A, and fig. S14E). Moreover, deleting the ETAA1 ATR-activation domain greatly reduced ATR activity in an unperturbed S phase but not in response to replication stress, while auxin-mediated degradation of a TOPBP1-mAID fusion had the opposite effect (Fig. 4, B and C and fig. S15). Thus, ETAA1 activates ATR during an unperturbed S phase, whereas TOPBP1-RAD9A activates ATR to enforce the replication stress response, providing a rationale for the existence of multiple ATR activators.

ATR enforces its checkpoint functions in part by activating CHK1, an effector kinase that inhibits CDKs (4). CHK1 inhibition also triggered premature FOXM1 phosphorylation and cyclin B accumulation (fig. S16, A-C). Thus, the repressive activity of a ETAA1-ATR-CHK1 pathway on the cyclin A-CDK1-FOXM1 axis controls the S/G2 transition (fig. S16D).

FOXM1 overexpression is sufficient to accelerate mitotic entry (10), therefore we asked whether ATR slows S-M progression by controlling FOXM1. Consistent with this hypothesis, reducing FOXM1 to levels that permit mitotic entry, while suppressing premature cyclin B expression in ATR-inhibited cells (fig. S7E), prevented ATRi-induced premature mitosis (Fig. 4, D and E). Furthermore, partial FOXM1 knockdown reduced ultrafine anaphase bridges (UFBs) and 53BP1 bodies following ATR inhibition (Fig. 4, F and G and fig. S17). As these both indicate a failure to complete DNA replication prior to mitosis (5, 15, 16), we conclude that

proper control of the S/G2 phosphorylation switch promotes the completion of DNA replication and prevents genome instability.

Our data unveil an ATR-controlled S/G2 phosphorylation switch that initiates the G2/M transcription program. By repressing CDK1, ATR blocks this switch until S phase ends to properly time G2-specific events. Although the molecular signal activating ATR in an unperturbed S phase is unclear, ETAA1's role suggests that ssDNA generated by ongoing replication, rather than unreplicated DNA, is a critical component. Transiently-formed RPA-coated ssDNA could serve as a platform for colocalizing ETAA1 and ATR, sustaining ATR activity throughout S phase. The decline in ATR activity that occurs once replication is complete then signals the S/G2 transition, executed via the CDK1-pFOXM1 switch (fig. S18).

Because ATR ensures that G2 depends on S phase completion, we refer to this as an intrinsic S/G2 checkpoint and propose this is a checkpoint that monitors replication completion (3). This checkpoint prevents a cellular identity crisis in which the S and G2 phases overlap, causing under-replication, early mitosis, and subsequent DNA damage. Given the frequent overexpression of FOXM1 in cancer (17), deregulation of this fundamental cell cycle transition could be a common event contributing to cancer genome instability.

References and Notes:

1. D. O. Morgan, *The cell cycle: principles of control*. Primers in biology (New Science Press Ltd in association with Oxford University Press, London, 2007), pp. xxvii, 297 p.
2. B. Lemmens *et al.*, DNA replication determines timing of mitosis by restricting CDK1 and PLK1 activation. *Mol Cell* **71**, 117-128 (2018).
3. S. J. Elledge, Cell cycle checkpoints: preventing an identity crisis. *Science* **274**, 1664-1672 (1996).
4. J. C. Saldivar, D. Cortez, K. A. Cimprich, The essential kinase ATR: ensuring faithful duplication of a challenging genome. *Nat Rev Mol Cell Biol*, (2017).

5. J. K. Eykelenboom *et al.*, ATR activates the S-M checkpoint during unperturbed growth to ensure sufficient replication prior to mitotic onset. *Cell Rep* **5**, 1095-1107 (2013).
6. S. Ruiz *et al.*, A Genome-wide CRISPR Screen Identifies CDC25A as a Determinant of Sensitivity to ATR Inhibitors. *Mol Cell* **62**, 307-313 (2016).
7. L. I. Toledo *et al.*, ATR prohibits replication catastrophe by preventing global exhaustion of RPA. *Cell* **155**, 1088-1103 (2013).
8. A. T. Hahn, J. T. Jones, T. Meyer, Quantitative analysis of cell cycle phase durations and PC12 differentiation using fluorescent biosensors. *Cell Cycle* **8**, 1044-1052 (2009).
9. K. Akopyan *et al.*, Assessing kinetics from fixed cells reveals activation of the mitotic entry network at the S/G2 transition. *Mol Cell* **53**, 843-853 (2014).
10. J. Laoukili *et al.*, FoxM1 is required for execution of the mitotic programme and chromosome stability. *Nat Cell Biol* **7**, 126-136 (2005).
11. S. Sadasivam, S. Duan, J. A. DeCaprio, The MuvB complex sequentially recruits B-Myb and FoxM1 to promote mitotic gene expression. *Genes Dev* **26**, 474-489 (2012).
12. J. Laoukili *et al.*, Activation of FoxM1 during G2 requires cyclin A/Cdk-dependent relief of autorepression by the FoxM1 N-terminal domain. *Mol Cell Biol* **28**, 3076-3087 (2008).
13. S. L. Spencer *et al.*, The proliferation-quiescence decision is controlled by a bifurcation in CDK2 activity at mitotic exit. *Cell* **155**, 369-383 (2013).
14. H. Hochegger *et al.*, An essential role for Cdk1 in S phase control is revealed via chemical genetics in vertebrate cells. *Journal of Cell Biology* **178**, 257-268 (2007).
15. K. L. Chan, T. Palmai-Pallag, S. Ying, I. D. Hickson, Replication stress induces sister-chromatid bridging at fragile site loci in mitosis. *Nat Cell Biol* **11**, 753-760 (2009).
16. C. Lukas *et al.*, 53BP1 nuclear bodies form around DNA lesions generated by mitotic transmission of chromosomes under replication stress. *Nat Cell Biol* **13**, 243-253 (2011).
17. J. Laoukili, M. Stahl, R. H. Medema, FoxM1: at the crossroads of ageing and cancer. *Biochim Biophys Acta* **1775**, 92-102 (2007).
18. J. D. Charrier *et al.*, Discovery of potent and selective inhibitors of ataxia telangiectasia mutated and Rad3 related (ATR) protein kinase as potential anticancer agents. *J Med Chem* **54**, 2320-2330 (2011).
19. T. E. Bass *et al.*, ETAA1 acts at stalled replication forks to maintain genome integrity. *Nat Cell Biol* **18**, 1185-1195 (2016).
20. A. R. Quinlan, I. M. Hall, BEDTools: a flexible suite of utilities for comparing genomic features. *Bioinformatics* **26**, 841-842 (2010).
21. K. Samejima *et al.*, Functional analysis after rapid degradation of condensins and 3D-EM reveals chromatin volume is uncoupled from chromosome architecture in mitosis. *J Cell Sci* **131**, (2018).
22. T. Natsume, T. Kiyomitsu, Y. Saga, M. T. Kanemaki, Rapid Protein Depletion in Human Cells by Auxin-Inducible Degron Tagging with Short Homology Donors. *Cell Rep* **15**, 210-218 (2016).

We thank F. Ochs, J Ferrell, and the Cimprich laboratory for comments on the manuscript.

Funding: This work was supported by grants from the NIH to K.A.C. (ES016486), D.C.

(CA102729) and T.M (GM127026), Wellcome Fund (107022 and 203149) to W.C.E., American Cancer Society (PF-15-165-01–DMC) and Burroughs Wellcome Fund Postdoctoral Enrichment Program to J.C.S., German Research Foundation DFG (HA 6996/1-1) to S.H., and Mexican Government CONACYT fellowship to F.C.-S. **Author Contributions:** J.C.S., W.C.E., D.C. K.S. and K.A.C. designed experiments. J.C.S., S.H., F.C.-S., K.S., J.R.P. L.X., T.E.B., and M.C. performed experiments. M.J.B. and M.C. performed the bioinformatics analyses. J.C.S., M.B., M.C., T.M., and K.A.C. analyzed the data. J.C.S. and K.A.C. wrote the manuscript. **Competing interests:** No competing interests to declare. **Data and materials availability:** RNA-seq data are available in the GEO repository (accession number GSE116131).

Figure Legends 1-4:

Figure 1. ATR represses a mitotic gene network during S phase. (A) S-M or G2-M

progression assay showing the cellular distribution at T=0 and gating scheme. See fig. S2 for details. **(B and C)**. Fraction of S- (B) or G2/M-gated (C) hTERT RPE-1 cells in mitosis as a function of time. Error bars represent SEM of n=3. **(D)** Experimental design and representative images of hTERT RPE-1 cells in G1, early to late S phase (S1-S4), G2, or mitosis. **(E)** QIBC plots of DNA content vs. EdU mean intensity, and mean cyclin B cytoplasmic intensity on a color scale. Boxes indicate gated populations used for analyses. **(F)** Mean cyclin B cytoplasmic intensities of gated populations from (E). Error bars represent SEM of n=4. **p < 0.05, ****p < 0.001. **(G)** RT-qPCR analysis of cyclin B1 mRNA from synchronized hTERT RPE-1 cells described in fig. S6. Error bars represent SEM from n=4. ***p < 0.01. **(H)** Unsupervised clustering analysis of mock or ATRi and early S, late S, or G2 synchronized cells (selected comparisons shown). Heatmap indicates the fold-change of normalized RNA-seq reads between

indicated samples (n=3). **(I)** Top 4 GO terms for Group 5 genes from (H). **(J)** Volcano plot of Log_{10} FDR-corrected p-values and log 2-fold change in gene expression of ATRi/mock of late S phase cells.

Figure 2. ATR controls an S/G2 FOXM1 phosphorylation switch. **(A)** Western blots of hTERT RPE-1 cells synchronized as in fig S6A. **(B)** Quantification of FOXM1 band intensities from (A) plotted as red lines (right y-axis). Black lines (left y-axis) represent the fraction of S phase synchronized cells, calculated as described in fig. S6, B-D. **(C)** Experimental design and representative images of S phase hTERT RPE-1 cells. **(D)** QIBC plots of DNA content vs. EdU mean intensity, and mean pFOXM1 T600 intensity on a color scale. Boxes indicate gated populations used for analyses. **(E)** Median pFOXM1 intensities from (D). Error bars represent SEM of n=4. **(F)** pFOXM1 T600 mean intensity in cells treated as described in (C). **(G)** QIBC plot of EdU-labeled cells with 4n DNA content. Boxes indicate gated populations used for analysis in (H). Numbers indicate cells in each gated population. S/G2 population determined as described in fig. S10. **(H)** pFOXM1 T600 mean intensity in indicated populations. In (F) and (H), whiskers indicate the 10th and 90th percentiles. Boxes indicate the 25th-75th percentile and median value.

Figure 3. ATR is active until G2, preventing CDK1-dependent FOXM1 phosphorylation.

(A) Experimental design and QIBC plots of DNA content vs. EdU mean intensity, and mean pFOXM1 T600 intensity on a color scale in hTERT RPE-1 cells. Boxes indicate gated populations used for analyses. **(B and C)** Median pFOXM1 intensities of populations shown in (A). Error bars represent SEM of n=3. **(D)** Representative images of indicated cell stage in

hTERT RPE-1 cells. **(E)** ATR activity during an unperturbed cell cycle as described in fig. S14. Error bars represent SEM of n=3.

Figure 4. The ETAA1-ATR pathway couples S phase and mitosis. **(A)** ATR activity in siRNA-transfected hTERT RPE-1 cells during an unperturbed cell cycle as described in fig. S14. Error bars represent the SEM of n=3 **(B)** Illustration of the mAID degron system fused to TOPBP1. **(C)** ATR activity in HCT116 cell lines mock-treated or auxin-treated (2 h) as described in fig. S15A. Error bars represent SEM of n=3. **(D and E)** S-M progression assay (see Fig. 1, A and B) in hTERT RPE-1 cells 40 h after siRNA transfection. Representative images 6 h post EdU-wash-off. **(E)** Fraction of S phase-gated cells in mitosis as a function of time post-EdU wash-off. Error bars represent SEM of n=3. **(F)** Representative images of anaphase cells 40 h after siRNA transfection and then mock- or ATRi-treated for 8 h. **(G)** Fraction of cells with UFBs. Error bars represent SEM of n=3.

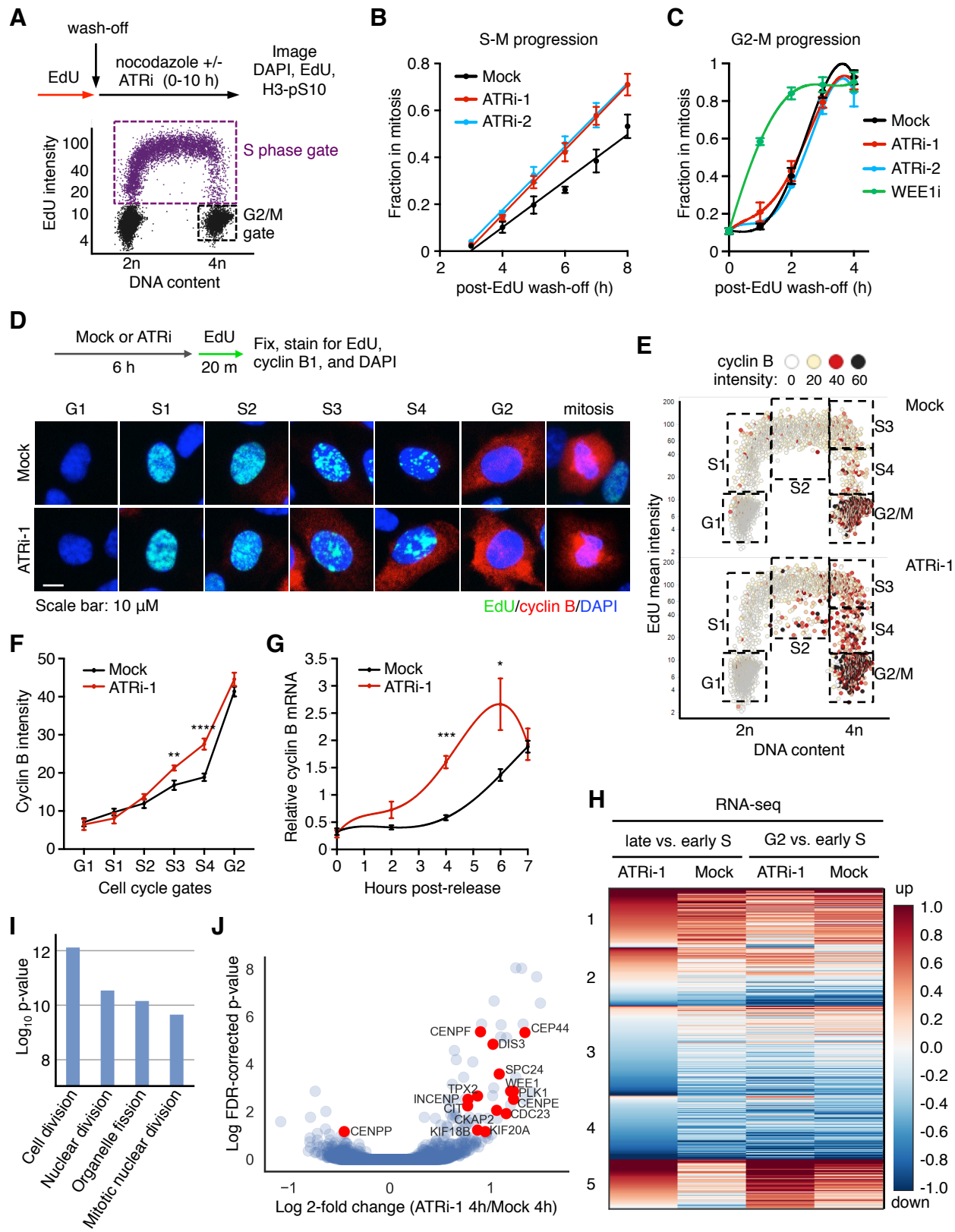
Fig. 1

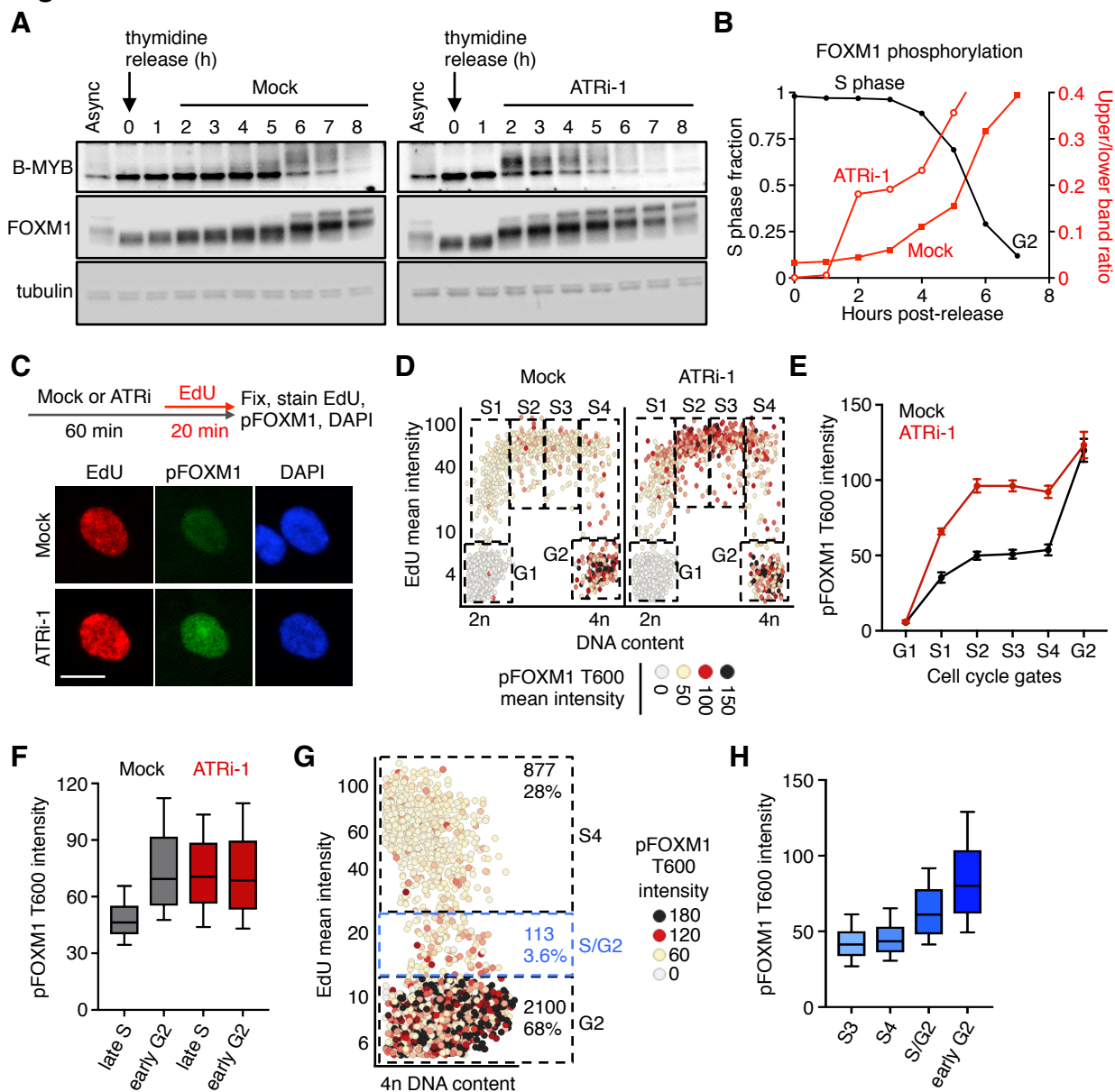
Fig. 2

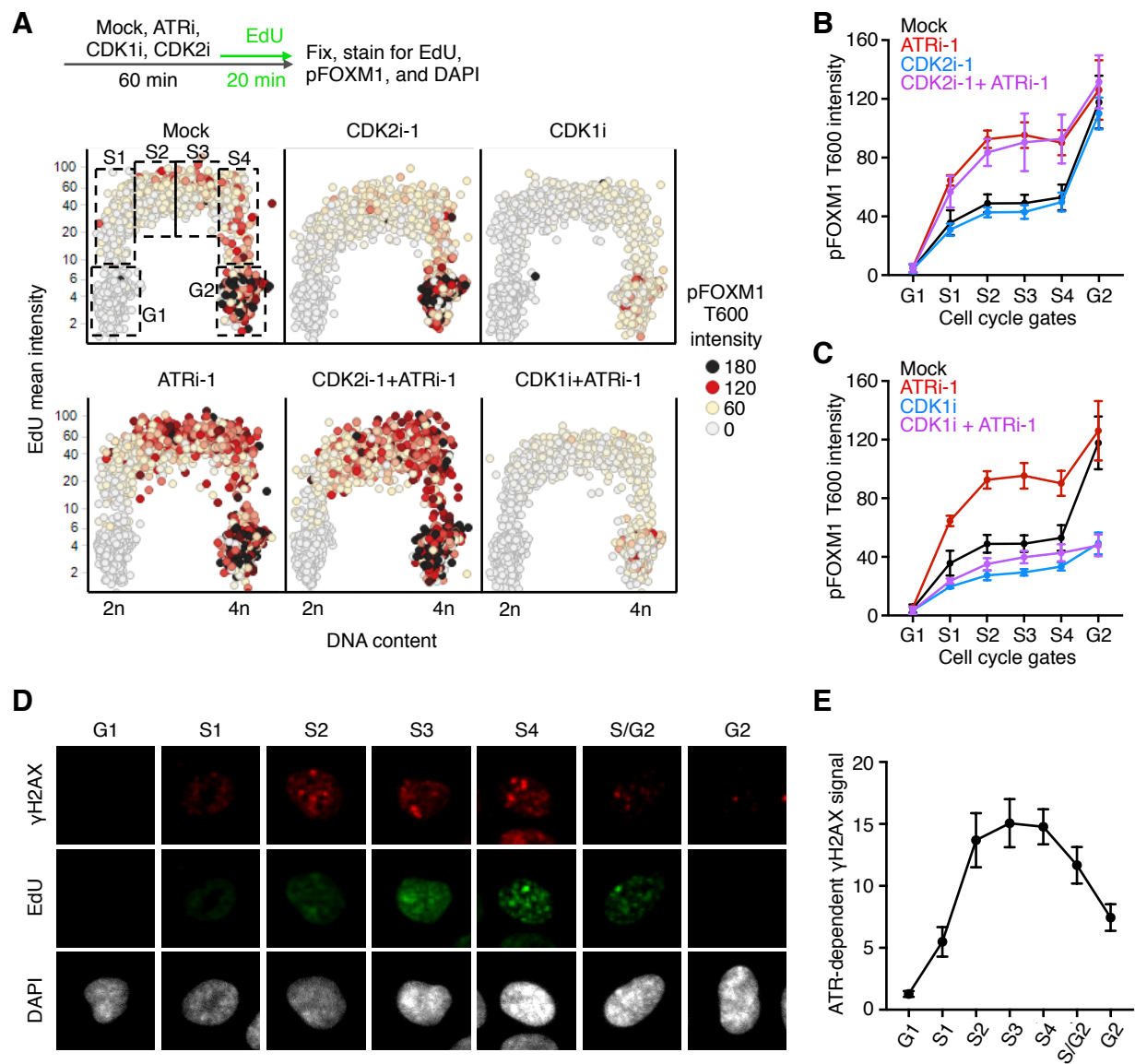
Fig. 3

Fig. 4

